

Magnetic fields produced by subsea high-voltage direct current cables reduce swimming activity of haddock larvae *Melanogrammus aeglefinus*

Alessandro Cresci , Caroline M. F. Durif, Torkel Larsen, Reidun Bjelland, Anne Berit Skiftesvik and Howard I. Browman

Institute of Marine Research, Austevoll Research Station, Sauganaset 16, N-5392 Storebø, Norway

*To whom correspondence should be addressed: Email: alessandro.cresci@hi.no

Edited By: Karen E. Nelson

Abstract

High-voltage direct current (HVDC) subsea cables are used to transport power between locations and from/to nearshore and offshore facilities. HVDC cables produce magnetic fields (B-fields) that could impact marine fish. Atlantic haddock (*Melanogrammus aeglefinus*) is a demersal fish that is at risk of exposure to anthropogenic B-fields. Their larvae drift over the continental shelf, and use the Earth's magnetic field for orientation during dispersal. Therefore, anthropogenic magnetic fields from HVDC cables could alter their behavior. We tested the behavior of 92 haddock larvae using a setup designed to simulate the scenario of larvae drifting past a B-field in the intensity range of that produced by a DC subsea cable. We exposed the larvae to a B-field intensity ranging from 50 to 150 μT in a raceway tank. Exposure to the B-field did not affect the spatial distribution of haddock larvae in the raceway. Larvae were categorized by differences in their exploratory behavior in the raceway. The majority (78%) of larvae were nonexploratory, and exposure to the artificial B-field reduced their median swimming speed by 60% and decreased their median acceleration by 38%. There was no effect on swimming of the smaller proportion (22%) of exploratory larvae. These observations support the conclusion that the swimming performance of nonexploratory haddock larvae would be reduced following exposure to B-field from HVDC cables. The selective impact on nonexploratory individuals, and the lack of impact on exploratory individuals, could have population-scale implications for haddock in the wild.

Keywords: subsea cables, renewable energy, offshore wind, anthropogenic magnetic field, fish larvae

Significance statement:

This study reports impacts of anthropogenic magnetic fields (B-fields) in the intensity range of those produced by high voltage direct current (DC) subsea cables on larval fish behavior. The findings have implications for marine spatial planning and engineering of marine renewable energy devices such as offshore wind farms. Atlantic haddock (*Melanogrammus aeglefinus*) larvae disperse through areas where DC subsea cables are present or planned, and impacts of anthropogenic magnetic fields could alter their dispersal. These results show that following exposure to anthropogenic B-fields, the swimming speed and acceleration of 78% of the tested haddock larvae are significantly reduced. The study also provides insights about magnetosensitivity in marine larval fish, which remains poorly understood.

Introduction

High-voltage direct Current (HVDC) subsea cables are used to transport electricity over long distances. They transport power between islands, connect islands to the coast, and transport electricity to/from nearshore and offshore structures, such as oil platforms and marine renewable energy devices (1, 2). HVDC cables are a valuable and cost-effective solution to support the expansion of offshore marine renewable energy facilities, including offshore wind farms (2, 3). The number and size of offshore wind facilities are increasing rapidly to meet the increasing demand for renewable energy (4, 5). HVDC cables have a relatively low loss over long distance and are expected to become the most used type of subsea cables connecting marine renewable energy devices (5).

When electricity moves through an HVDC subsea cable, it generates a static magnetic field (B-field) in the proximity of the cable (6, 7). HVDC-induced B-field intensity varies with the power being transmitted through the cable and with the type of cable (8). The B-field intensity, which can reach 100 s of microtesla (μT) (2, 6), extends radially from the cable, and is highest at the cable surface, decreasing inversely with distance from it (7, 8). However, the decrease in magnetic field intensity with distance from the cable is nonlinear; it drops off sharply (7, 8). Due to the development of offshore sectors such as renewable energy facilities, the number and length of HVDC cables associated with marine renewable energy devices will increase, causing concern over potential effects that the exposure to anthropogenic B-fields could have on marine

Competing interest: The authors declare no competing interest.

Received: April 29, 2022. **Accepted:** August 25, 2022

© The Author(s) 2022. Published by Oxford University Press on behalf of the National Academy of Sciences. This is an Open Access article distributed under the terms of the Creative Commons Attribution-NonCommercial-NoDerivs licence (<https://creativecommons.org/licenses/by-nc-nd/4.0/>), which permits non-commercial reproduction and distribution of the work, in any medium, provided the original work is not altered or transformed in any way, and that the work is properly cited. For commercial re-use, please contact journals.permissions@oup.com

organisms residing near, or drifting by, subsea cables (3, 6), since anthropogenic B-fields can impact behaviors that influence spatial distribution, such as swimming and orientation (9). For marine fish, the risk of exposure is particularly relevant during the early life stages, when fish have limited swimming capacity and they are still developing.

Several marine fish can sense the Earth's geomagnetic field and use it to orient during migration, including during the larval stages (10–12). Impacts of B-fields on larval swimming or orientation behavior would have consequences for their dispersal (13, 14), with possible downstream effects on survival and recruitment (15). The expansion of renewable energy facilities further offshore, with a concomitant increase in the length and number of subsea cables, increases the risk of exposure to anthropogenic B-fields for dispersing fish larvae. Previous studies demonstrated that anthropogenic B-fields and electromagnetic fields can alter the swimming and spatial distribution of marine species (16–18). However, there is very limited knowledge on the possible effects of B-fields from anthropogenic sources (such as HVDC) on the behavior of marine fish larvae that reside in, or disperse through, areas where HVDC is present.

Atlantic haddock (*Melanogrammus aeglefinus*) is a species of commercial and ecological importance in Europe (19). One of its largest stocks is located in the North Sea (20). Larval and juvenile habitats for haddock are associated with the continental shelf (21). In the North Sea, haddock larvae disperse for a period of 2 to 3 months in mid-water and close to the sea bottom (21, 22), in areas where facilities connected by HVDC cables (such as offshore wind farms) are operating or are planned (<https://www.equinor.com/no/what-we-do/floating-wind.html>). Moreover, haddock larvae are magneto-sensitive and use the geomagnetic field to guide their horizontal swimming at sea, relying on a magnetic compass mechanism for orientation (11). For all of these reasons, Atlantic haddock are at risk of being impacted by anthropogenic B-fields generated by HVDC cables. Whether B-fields generated by HVDC subsea cables affect the swimming behavior and spatial distribution of Atlantic haddock larvae is unknown.

We conducted an experiment on Atlantic haddock larvae to assess the potential impact of static magnetic fields in the intensity range of those emitted by HVDC subsea cables. We used an electric coil system to modify the B-field in a manner that simulated the scenario of fish larvae swimming or drifting through a B-field in the intensity range of that produced by a DC subsea cable. We tested the null hypothesis that an artificially modified B-field where a high-intensity area is followed by a sharp drop in intensity toward a low-intensity area has no impact on spatial distribution or swimming behavior of Atlantic haddock larvae.

Methods

Experimental animals

Haddock broodstock were collected locally from the waters near Austevoll (60.085 N, 5.261 E), Norway and two females were used as the source of eggs, which were then fertilized. Eggs were placed into one 500 L tank at a density of 100 eggs/L. Water exchange was set at 4 L/min. During the spring at high latitudes, larvae have enough light to feed at sea for most of the day. Thus, the photoperiod was set to 24 h under 2 × 25 w, 12 V halogen lamps. The larvae were reared in green water (*Nannochloropsis*, Reed Mariculture) at a temperature of 11 to 12°C and a salinity of ca. 35 PSU. Larvae were fed first on a diet of rotifers (*Brachionus* sp.) and natural plankton (mainly *Acartia nauplii*), and then (25 days post hatch) on *Artemia* and natural plankton copepod (primarily

Acartia sp.). Eggs hatched on 2021 March 19 and larvae started feeding on March 22.

Ninety-two larvae were used in the experiments on larval behavior. The larvae were 31 to 33 days post hatch and were 8.2 ± 1.2 mm standard length (mean \pm SD). Developmentally, larvae were at the beginning of the flexion stage, which in haddock occurs at approximately 10 mm standard length (23).

Experimental setup and exposure to B-field

The experimental setup used in this study was designed to expose Atlantic haddock larvae to a B-field in the intensity range of that produced by a DC subsea cable (Fig. 1), and followed the outline of the setup described in (24, 25). To accomplish this, we used two square Helmholtz coils (65 × 65 cm; 30 wraps of copper wire for each coil) connected to a BK Precision 1745 A DC power supply (0 to 10 A), and generated a B-field intensity (50 to 150 μ T) in a tank with two separate raceways (Fig. 1) (24). The raceway tank was produced using a 3D printer (Ultimaker Cura S5—material white Tough PLA) (24), and was placed halfway inside the coils and filled with filtered seawater (Fig. 1A) (24). With the raceway positioned in this way, running a current through the coils generated a high B-field intensity on side 1 of the raceways, and a low B-field intensity on side 2 (see Fig. 1B) (24). The B-field was highest (150 μ T) on one side of the raceway, sharply dropped in intensity, and was lowest at the other end of the raceway (approximately 50 μ T). A similar pattern in B-field intensity is found in proximity of DC subsea cables (7, 26). The B-field intensities produced were also in the range of those produced by HVDC subsea cables associated with facilities such as offshore wind farms (2, 6). The experimental coils were parallel to the ground and modified the vertical component of the geomagnetic field, which had a total intensity (F) of 50 μ T (73° Inclination and deviation of <1°) (24). The intensity of the B-field was recorded using a MLX90393 Triaxis Magnetic Node magnetometer from Melexis Inspired Engineering (Belgium) (24).

Larvae could swim freely from the high to the low B-field intensity area and vice versa in the raceway—50 cm long, 7 cm wide, and 3.5 cm deep. To minimize possible attraction-aggregation areas, the raceway was designed so that there were no sharp edges and the corners were rounded (Fig. 1A) (24). All the experiments were conducted in the dark to eliminate any possible visual cues for the larvae. A GOPRO HERO 7, modified for night vision and positioned above the raceway looking down onto it, was used to video record fish larvae during the experiments. The two DC 12 V 96 LED infrared illuminators were placed beside the camera. The room temperature was set at 11°C, which was the same temperature as the water in the rearing tanks of the larvae (24).

Behavioral observations and data analysis

The experiment, and all handling of animals at the start/end of every test, was conducted in the dark. This was to minimize the exposure to any other external cue other than the magnetic field. The day of the experiment, larvae were transferred in filtered seawater in 6.3 L tanks at a density of 3 larvae/L. The tanks were in the dark. Larvae were transferred to the dark tanks 1 h before the experiments (24). Larvae were tested individually. A single larva was placed in the middle of the raceway using a small cup and was allowed 5 min to acclimate to the raceway, after which its behavior was recorded for 10 min. To eliminate possible disturbance to the larva in the raceway tank, the observer started and stopped the GOPRO recording from outside the room using a remote control (24).

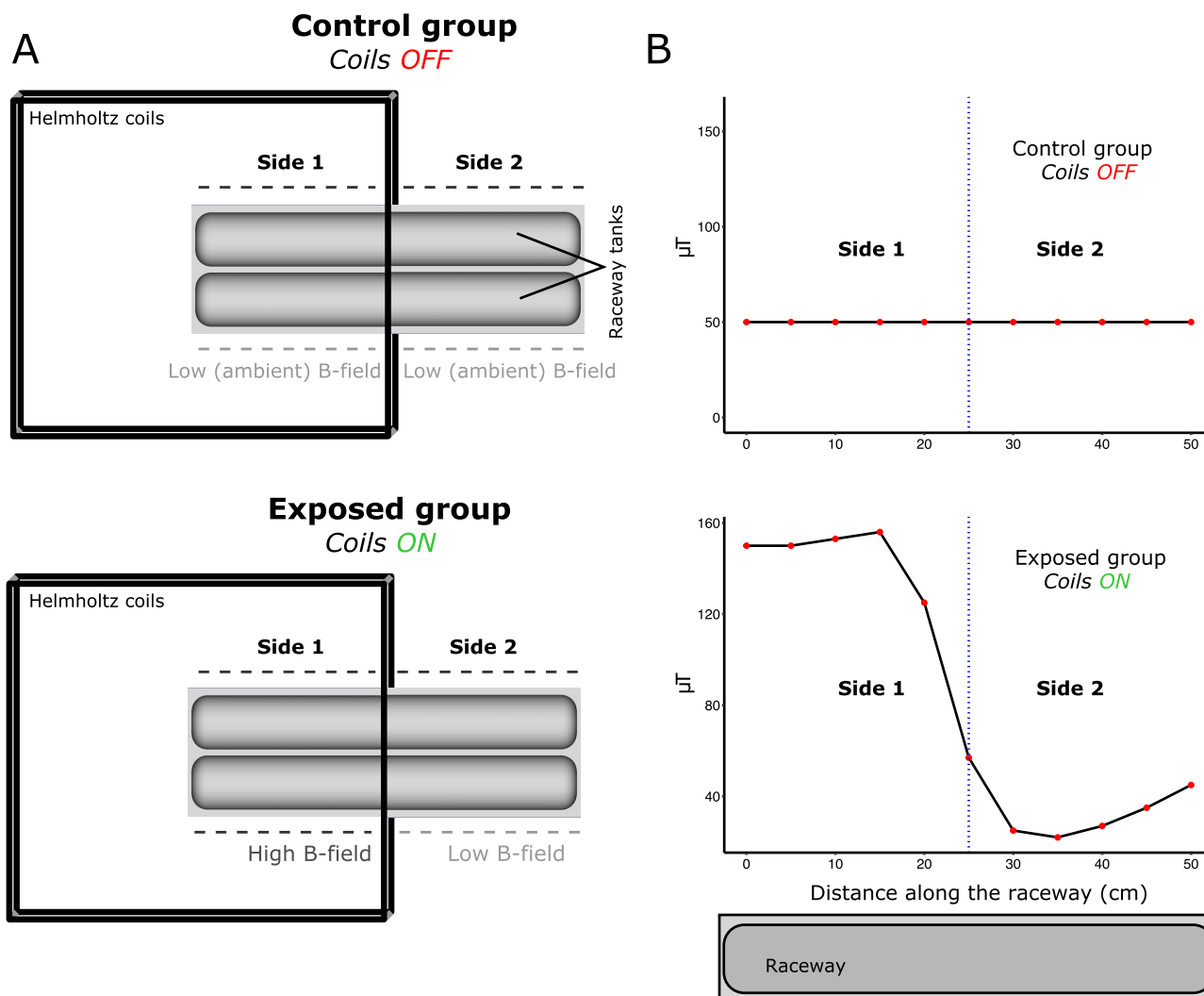


Fig. 1. (A) Experimental setup (top view) used to expose Atlantic haddock (*M. aeglefinus*) larvae to a static magnetic field (B-field) gradient. The black squares are a pair of parallel Helmholtz coils. The two gray rectangles with smoothed corners are two raceways in which larvae were swimming. Black dashed lines show the two sides of the raceway (side 1 inside the coils; side 2 outside the coils). Light and dark gray dashed lines show the intensity of the B-field on each side of the raceway. In the Control group (coils OFF), there was an ambient geomagnetic field in both sides of the raceway. In the Exposed group (coils ON), there was higher B-field intensity on side 1, and lower intensity (close to the geomagnetic field intensity) on side 2. (B) B-field intensity along the raceway (x-axis) with coils ON and coils OFF. In the Control group, the geomagnetic field had the same value along the whole raceway (50 μT). In the Exposed group, the B-field intensity had a gradient going from 150 μT on Side 1, decreasing toward the end of side 2, to settle at approximately 50 μT at the right end of half 2. Haddock larvae were free to swim along the whole raceway during the experiment. Figure modified from Cresci et al., 2022 (24).

We replicated the protocol for one larva at a time in each of the two raceways, replacing the larvae with new individuals at the end of each 15 min test (Fig. 1A). A total of 92 haddock larvae were tested. Half of these (Controls, $N = 46$ replicates) were video recorded in the raceway with the electric coils switched OFF (Fig. 1). The other half of the larvae (Exposed, $N = 46$ replicates) were recorded with the coils switched ON and were, therefore, exposed to a B-field intensity ranging from 50 to 150 μT with a sharp drop in intensity in the middle of the raceway (Fig. 1B) (24).

Atlantic haddock larvae in the videos were tracked manually using Tracker 5.1.5. (Copyright© 2020 Douglas Brown, <https://physlets.org/tracker>). We tracked the position of each larva, every second, for the 10-min observation period (600 data points per haddock larva) (24). The tracks were used to calculate the position of larvae along the raceway and to measure their swimming kinematics (median and maximum speed, and acceleration) (24).

Data on fish length, position along the x-axis, and median and maximum swimming speed and acceleration were tested for normality using the Shapiro-Wilk test. As data were not normally distributed, comparisons between experimental groups (B-field ON and OFF) were conducted using the nonparametric Wilcoxon test. Values for each group are reported as median (Inter Quartile Range; IQR).

Results

Behavior of Atlantic haddock larvae in the raceway

Individual Atlantic haddock larvae exhibited distinct interindividual differences in exploratory and swimming behavior. After the 5-min habituation period, 20 out of 92 larvae (22%) were actively swimming along the raceway without settling on either

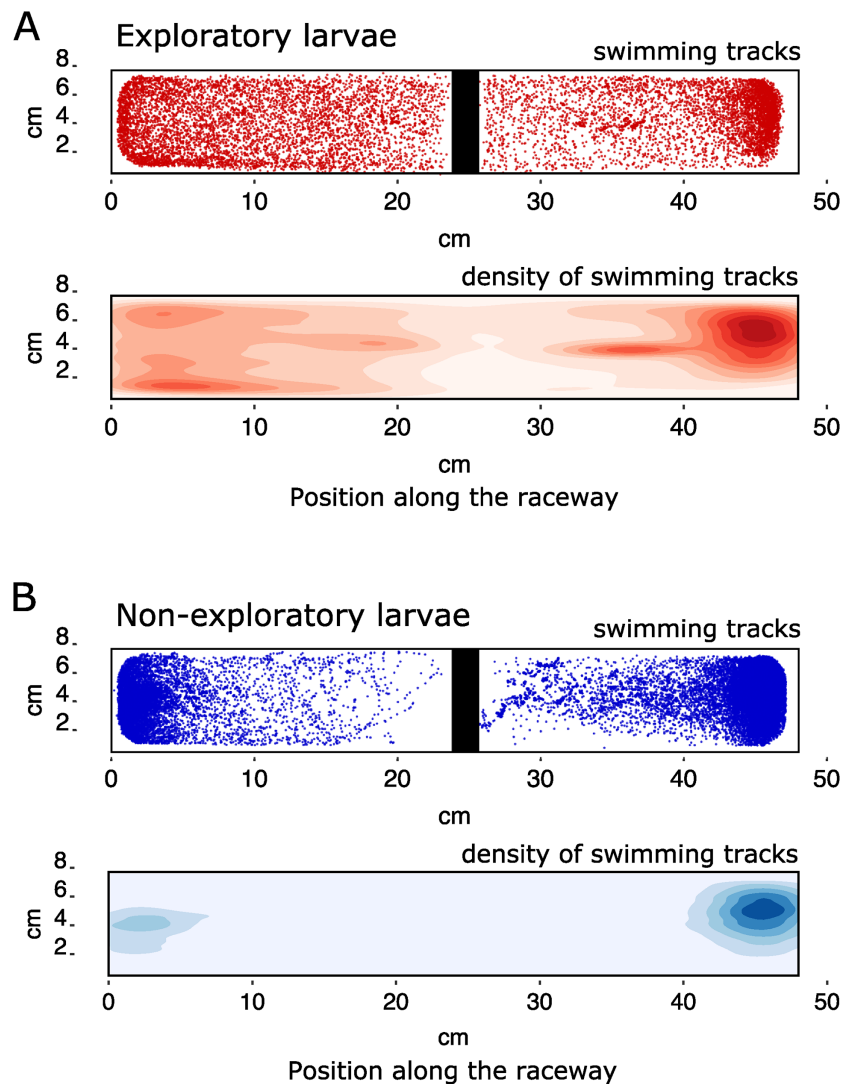


Fig. 2. Swimming tracks of Atlantic haddock (*M. aeglefinus*) larvae. The black rectangle represents the raceway. The vertical dark rectangle in the middle of the raceway represents the electric coil passing between the camera and the raceway. (A) Tracks of exploratory haddock larvae recorded every second, and density of the tracks in the raceway. The density is calculated as a 2D kernel density estimation on a square grid (function `geom_density_2d_filled`, `ggplot2` package, R). (B) Tracks of nonexploratory haddock larvae and density of the tracks in the raceway.

side, exploring the entire space available to them (Fig. 2A). These larvae crossed the middle of the raceway at least once during the 10-min-long test and were categorized as “exploratory.” The rest of the larvae, which represented the majority of the individuals (72 out of 92; 78%), settled on one of the two sides of the raceway and never crossed the middle of it during the test (Fig. 2B). These larvae were categorised as “nonexploratory” (Fig. 2B).

Exploratory larvae had a median speed of 0.92 (0.54) cm/s [median (IQR)], which was significantly higher ($W = 1259.5$, $P < 0.01$) than the median speed of 0.27 (0.42) cm/s displayed by nonexploratory larvae. During the 10 min observation period, exploratory larvae swam on average 6.3 ± 3.2 m (mean \pm SD), while nonexploratory fish swam on average 2.3 ± 1.4 m. Exploratory larvae had median standard length of 9.0 (1.5) mm, which was significantly greater ($W = 1170$, $P = 0.38$) than the median length of 7.8 (1.3) mm of nonexploratory individuals.

Impact of B-field

Exposure to B-field did not affect the spatial distribution (position along the x-axis of the raceway) of larvae along the raceway ($W = 634$, $P = 0.89$). Nor was there an effect of B-field on spatial distribution when exploratory larvae ($W = 41$, $P = 0.62$) or nonexploratory larvae ($W = 634$, $P = 0.90$) were assessed as categories.

The swimming speed of Exposed nonexploratory larvae ($N = 34$, median = 0.13 cm/s, IQR = 0.36) was 60% lower than the median speed of Control nonexploratory larvae ($N = 38$, median = 0.34 cm/s, IQR = 0.31) ($W = 862$, $P = 0.01$) (Fig. 3A). B-field Exposed nonexploratory larvae also had significantly lower acceleration ($W = 844.5$, $P = 0.02$) ($N = 34$, median = 0.09 cm/s², IQR = 0.17) compared to Control nonexploratory larvae ($N = 38$, median = 0.15 cm/s², IQR = 0.14) (Fig. 3B). Median speed and acceleration of exploratory larvae were unaffected by exposure to B-field (Wilcox. $P > 0.05$) (Fig. 3A and B). Exposure to B-field did not impact the maximum swimming speed (Fig. 3C) and maximum acceleration (Fig. 3D) of exploratory and nonexploratory larvae

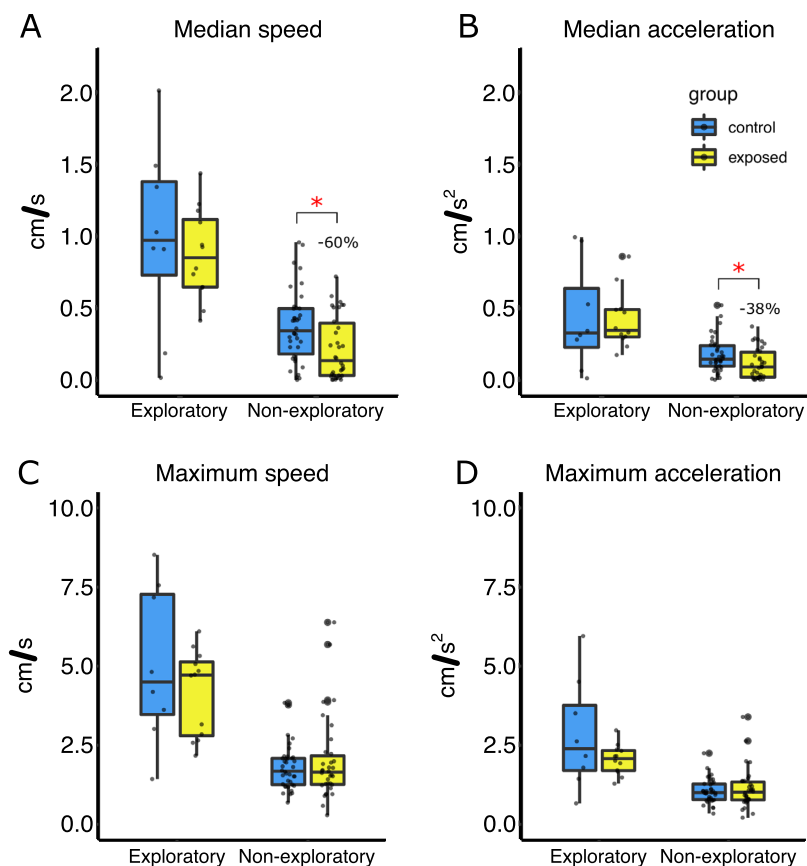


Fig. 3. Swimming speed and acceleration of Atlantic haddock (*M. aeglefinus*) larvae in the raceway (Control and Exposed to magnetic field). Boxplots show minimum, 25th percentile, median, 75th percentile, and maximum values. Data points in the boxplots show the value for each individual larva and are separated out along the x-axis for visualization purposes only (to avoid overlap). Red asterisks show statistically significant differences ($\alpha = 0.05$) between Control and Exposed larvae. Data are displayed according to the exploratory behavior of haddock larvae (Exploratory; Nonexploratory). (A) Median speed. (B) Median acceleration. (C) Maximum speed. (D) Maximum acceleration.

(Wilcox. $P > 0.05$). Data are available in the Supplementary Material file.

Discussion

A simulated static B-field of intensity ranging between 50 and 150 μT did not influence the spatial distribution of Atlantic haddock larvae (*M. aeglefinus*) in a raceway. B-field exposure did not cause attraction to either side of the raceway. These findings suggest that haddock larvae would not actively swim toward or away from B-fields in the intensity range of those produced by HVDC cables. However, more research is needed to address whether haddock larvae would be attracted to or repelled from HVDC cables in situ.

Exposure to B-field in the intensity range of that produced by subsea DC cables did not affect the behavior of all haddock larvae equally. The effect depended upon interindividual variability in exploratory behavior (Figs. 2 and 3). Specifically, haddock larvae exhibited two distinct exploratory behaviors after being introduced into the raceway (Fig. 2): exploratory larvae (22% of the total number of individuals observed) explored the whole space available to them and displayed much higher swimming speeds compared to nonexploratory larvae (which were 78% of the total number of individuals observed). Exposure to a B-field intensity in the range of that produced by HVDC cables reduced the swimming

speed of nonexploratory haddock larvae by 60% and their acceleration by 38% (Fig. 3). This suggests that nonexploratory haddock larvae drifting in proximity of HVDC subsea cables would swim slower if exposed to these B-field levels. Exposure to B-field had no effect on the swimming of exploratory haddock larvae. However, this could be due to the smaller sample size of that group ($n = 20$) that might have been insufficient to identify a B-field-related difference in swimming speed.

Although exploratory larvae were the same age as nonexploratory larvae, they were significantly larger by 0.8 mm (on average). This difference might account for part of the difference in speed between exploratory and nonexploratory larvae. Exploratory larvae had a median speed of 0.92 cm/s, which was 240% higher than the median speed of nonexploratory larvae. Gadoid larvae 4.5 to 9.5 mm long display an increase in routine swimming speed of $\sim 35\%$ within each 1 mm increase in total body length (27). Thus, the large difference in swimming speed between exploratory and nonexploratory larvae observed in this study is likely to depend on interindividual differences in locomotory activity rather than on a difference in body size.

The differences in exploratory behavior reported in this study, as well as the proportion of individuals in each category, are consistent with literature categorizing individual fish based on differences in locomotory activity and exploratory behavior as “proactive” and “reactive” (28, 29). Proactive–reactive differences have

been reported in many fish species, such as zebrafish (*Danio rerio*) (30), cod (*Gadus morua*) (29), northern pike (*Esox lucius*) (31), and gilthead seabream (*Sparus aurata*) (32). Proactive–reactive differences in behavior have also been reported during the larval stages in fish (31). Most of the haddock larvae (78%) observed in the raceways could be considered reactive individuals. This is consistent with other studies in which reactive individuals typically predominate (>70%) (33); (34); (29). The higher sensitivity to B-fields displayed by nonexploratory larvae is consistent with previous work showing that reactive fish respond to changes in B-field intensity and direction, but proactive fish do not (33, 35). This selective impact of B-field could have important implications for cohorts of larvae interacting with subsea cables, as reactive fish tend to be risk-averse (36) and are more adaptable to changes in the environment (37).

A reduction in swimming activity could have consequences for the dispersal ecology of this species because it would decrease the active swimming component of their horizontal drifting trajectory, increasing the relative importance of passive transport (powered by ocean currents) (13, 14, 38). This might alter the spatial distribution of haddock larvae, which could result in them drifting to different areas, potentially areas with less food and more predation compared to their usual dispersal routes and nursery areas (15). In addition, Atlantic haddock larvae are magneto-sensitive: anthropogenic B-field could alter their drifting trajectory by interfering with the magnetic compass that they use to orient *in situ* (11). Whether exposure to B-field from HVDC cables has long-term impacts on the magnetic orientation abilities of haddock larvae has yet to be investigated.

The observed effects of exposure to static B-field on haddock larvae are consistent with those reported for other marine species (9). High-intensity B-field (2.8 mT) affected the spatial distribution of the crab *Cancer pagurus*, which was attracted to areas with strong B-field intensity (39). Similarly, exposure to small increases in B-field intensity (10 μ T higher than the background geomagnetic field) influenced electrosensitive fish, such as the little skate *Leucoraja erinacea*, which spent less time in the center of an experimental arena when exposed to altered B-field (16). However, not all aquatic species are affected by changes in B-field. For example, B-fields (up to 200 μ T) did not affect spatial preference and shelter-seeking behavior in juvenile European lobsters (*Homarus gammarus*) (25). Similarly, rainbow trout (*Oncorhynchus mykiss*) juveniles did not show direct avoidance of either static or time varying strong B-field of 10 mT (40).

Future work should investigate how long the effects of exposure to B-field last and on estimating the threshold of B-field intensity, causing impacts on haddock larvae. That additional information would support estimating a risk area around facilities that are connected to HVDC subsea cables. Future research should investigate movement patterns of later life stages of Atlantic haddock around subsea cables using high-resolution acoustic telemetry technology. This approach would provide details on the habitat use of this species (41) in areas where subsea cables are planned and, later, be compared to when they are present.

Acknowledgments

Thanks to Stig Ove Utskot for carefully and successfully rearing the haddock larvae used in this study.

Ethical Statement

The Austevoll Research Station has a permit to operate as a Research Animal facility for fish (all developmental stages), under

code 93 from the national Institutional Animal Care and Use Committee (IACUC); NARA. We did not require specific approval for these experiments because they are behavioral observations of a nonintrusive potential stimulus.

Conflict of Interest

The authors declare no conflict of interest.

Supplementary Material

Supplementary material is available at *PNAS Nexus* online.

Funding

This work was funded by the Norwegian Institute of Marine Research's project "Assessing the effects of offshore wind power generating facilities on the early life stages of fish" (project # 15655) to H.I.B.

Authors' Contributions

A.C. designed the study, collected, analyzed, and interpreted the data, and wrote the paper. C.M.F.D. designed the study, interpreted the data, and wrote the paper. T.L. analyzed, and interpreted the data. R.B. designed the study, interpreted the data, and wrote the paper. A.B.S. designed the study, interpreted the data, and wrote the paper. H.I.B. designed the study, interpreted the data, wrote the paper, and is the leader of the project that funded the research.

Data Availability

All data are included in the manuscript and/or supporting information.

References

1. Sutton SJ, Lewin PL, Swingler SG. 2017. Review of global HVDC subsea cable projects and the application of sea electrodes. *Int J Electr Power Energy Syst.* 87: 121–135.
2. Taormina B, et al. 2018. A review of potential impacts of submarine power cables on the marine environment: knowledge gaps, recommendations and future directions. *Renew Sustain Energy Rev.* 96:380–391.
3. Hutchison ZL, Secor DH, Gill AB. 2020b. The interaction between resource species and electromagnetic fields associated with electricity production by offshore wind farms. *Oceanography.* 33:96–107.
4. deCastro M, et al. 2019. Europe, China and the United States: three different approaches to the development of offshore wind energy. *Renew Sustain Energy Rev.* 109: 55–70.
5. Soares-Ramos EPP, de Oliveira-Assis L, Sarrias-Mena R, Fernández-Ramírez LM. 2020. Current status and future trends of offshore wind power in Europe. *Energy.* 202: 117787.
6. Gill A, Desender M. 2020. 2020 State of the Science Report, Chapter 5: Risk to Animals from Electromagnetic Fields Emitted by Electric Cables and Marine Renewable Energy Devices. Richland, (WA) USA <https://doi.org/10.2172/1633088>
7. Hutchison ZL, Gill AB, Sigra P, He H, King JW. 2021. A modelling evaluation of electromagnetic fields emitted by buried subsea power cables and encountered by marine animals: considerations for marine renewable energy development. *Renew Energy.* 177:72–81.

8. Yang C et al. 2018. Simulation and analysis of magnetic field in HVDC transmission cable. IOP Conf Ser Mater Sci Eng. 382:032041.
9. Nyqvist D, et al. 2020. Electric and magnetic senses in marine animals, and potential behavioral effects of electromagnetic surveys. Mar Environ Res. 155:104888.
10. Bottesch M, et al. 2016. A magnetic compass that might help coral reef fish larvae return to their natal reef. Curr Biol. 26:R1266–R1267.
11. Cresci A, et al. 2019. Atlantic haddock (*Melanogrammus aeglefinus*) larvae have a magnetic compass that guides their orientation. *Iscience*. 19:1173–1178.
12. O'Connor J, Muheim R. 2017. Pre-settlement coral-reef fish larvae respond to magnetic field changes during the day. J Exp Biol. 220:2874–2877.
13. Cresci A, et al. 2021. The lunar compass of European glass eels (*Anguilla anguilla*) increases the probability that they recruit to North Sea coasts. Fish Oceanogr. 30:315–330.
14. Fiksen Ø, Jørgensen C, Kristiansen T, Vikebø F, Huse G. 2007. Linking behavioural ecology and oceanography: larval behaviour determines growth, mortality and dispersal. Mar Ecol Prog Ser. 347:195–205.
15. Houde ED. 2016. In: Recruitment variability. Jakobsen T, Fogarty MJ, Megrey BA, Moksness E, editors. Fish reproductive biology: implications for assessment and management. The Atrium Southern Gate Chichester West Sussex, PO19 8SQ United Kingdom: John Wiley & Sons, Ltd. p. 98–187.
16. Hutchison ZL, Gill AB, Sigray P, He H, King JW. 2020a. Anthropogenic electromagnetic fields (EMF) influence the behaviour of bottom-dwelling marine species. Sci Rep. 10:1–15.
17. Westerberg H, Lagenfelt I. 2008. Sub-sea power cables and the migration behaviour of the European eel. Fish Manag Ecol. 15:369–375.
18. Wyman MT, et al. 2018. Behavioral responses by migrating juvenile salmonids to a subsea high-voltage DC power cable. Mar Biol. 165:134.
19. Pope J, Macer CT. 1996. An evaluation of the stock structure of North Sea cod, haddock, and whiting since 1920, together with a consideration of the impacts of fisheries and predation effects on their biomass and recruitment. ICES J Mar Sci. 53:1157–1169.
20. Daan N, Bromley PJ, Hislop JRG, Nielsen NA. 1990. Ecology of North Sea fish. Neth J Sea Res. 26:343–386.
21. Albert O. 1994. Ecology of haddock (*Melanogrammus aeglefinus* L.) in the Norwegian Deep. ICES J Mar Sci. 51:31–44.
22. Munk P, Larsson P, Danielssen D, Moksness E. 1999. Variability in frontal zone formation and distribution of gadoid fish larvae at the shelf break in the northeastern North Sea. Mar Ecol Prog Ser. 177:221–233.
23. Auditore PJ, Lough RG, Broughton EA. 1994. A review of the comparative development of Atlantic cod (*Gadus morhua* L.) and haddock (*Melanogrammus aeglefinus* L.) based on an illustrated series of larvae and juveniles from Georges Bank. NAFO Sci Council Stud. 20:7–18.
24. Cresci A, et al. 2022. Magnetic fields generated by the DC cables of offshore wind farms have no effect on spatial distribution or swimming behavior of lesser sandeel larvae (*Ammodytes marinus*). Mar Environ Res. 176:105609.
25. Taormina B, et al. 2020. Impact of magnetic fields generated by AC/DC submarine power cables on the behavior of juvenile European lobster (*Homarus gammarus*). Aquat Toxicol. 220:105401.
26. Dhanak M, et al. 2016. Assessment of electromagnetic field emissions from Subsea cables. Paper Presented at: The 4th Marine Energy Technology Symposium; Washington (DC), USA. https://doi.org/10.0/Linux-x86_64
27. Peck MA, Buckley LJ, Bengtson DA. 2006. Effects of temperature and body size on the swimming speed of larval and juvenile Atlantic cod (*Gadus Morhua*): implications for individual-based modelling. Environ Biol Fishes. 75:419–429.
28. Baker MR, Goodman AC, Santo JB, Wong RY. 2018. Repeatability and reliability of exploratory behavior in proactive and reactive zebrafish, *Danio rerio*. Sci Reports. 8:1–9.
29. Villegas-Ríos D, Réale D, Freitas C, Moland E, Olsen EM. 2018. Personalities influence spatial responses to environmental fluctuations in wild fish. J Anim Ecol. 87:1309–1319.
30. Tudorache C, Schaaf MJM, Slabbekoorn H. 2013. Covariation between behaviour and physiology indicators of coping style in zebrafish (*Danio rerio*). J Endocrinol. 219:251–258.
31. Pasquet A, et al. 2015. First insight into personality traits in Northern pike (*Esox lucius*) larvae: a basis for behavioural studies of early life stages. Environ Biol Fishes. 99:105–115.
32. Castanheira MF, et al. 2016. Are personality traits consistent in fish? The influence of social context. Appl Anim Behav Sci. 178:96–101.
33. Cresci A, et al. 2018. Zebrafish “personality” influences sensitivity to magnetic fields. Acta Ethol. 21:195–201.
34. Rey S, Boltana S Vargas RMackenzie S. 2013. Combining animal personalities with transcriptomics resolves individual variation within a wild-type zebrafish population and identifies underpinning molecular differences in brain function. Molecular Ecology. 22 (24):6100–6115. <https://doi.org/10.1111/mec.12556>
35. Cresci A, De Rosa R, Agnisola C. 2019. Assessing the influence of personality on sensitivity to magnetic fields in zebrafish. J Vis Exp. 145:e59229. <https://doi.org/10.3791/59229>
36. Ibarra-Zatarain Z, Parati K, Cenadelli S, Duncan N. 2019. Reproductive success of a marine teleost was correlated with proactive and reactive stress-coping styles. J Fish Biol. 94:402–413.
37. Carbonara P, et al. 2019. Behavioral and physiological responses to stocking density in sea bream (*Sparus aurata*): do coping styles matter? Physiol Behav. 212:112698.
38. Vikebø FB, et al. 2011. Real-time ichthyoplankton drift in north-east Arctic Cod and Norwegian spring-spawning herring. PLoS One. 6:e27367.
39. Scott K, Harsanyi P, Lyndon AR. 2018. Understanding the effects of electromagnetic field emissions from Marine Renewable Energy Devices (MREDS) on the commercially important edible crab, *Cancer pagurus* (L.). Mar Pollut Bull. 131:580–588.
40. Jakubowska M, et al. 2021. Effects of magnetic fields related to submarine power cables on the behaviour of larval rainbow trout (*Oncorhynchus mykiss*). Mar Freshwater Res. 72:1196–1207.
41. Nathan R, et al. 2022. Big-data approaches lead to an increased understanding of the ecology of animal movement. Science. 375:eabg1780.